Chemical Science

ROYAL SOCIETY OF CHEMISTRY

EDGE ARTICLE

View Article Online
View Journal | View Issue

Cite this: *Chem. Sci.*, 2022, **13**, 4801

All publication charges for this article have been paid for by the Royal Society of Chemistry

Stereodivergent synthesis of enantioenriched azepino[3,4,5-*cd*]-indoles *via* cooperative Cu/Ir-catalyzed asymmetric allylic alkylation and intramolecular Friedel–Crafts reaction†

Lu Xiao,‡[ab] Bo Li,‡[c] Fan Xiao,[a] Cong Fu,[a] Liang Wei,[a] Yanfeng Dang,*[c] Xiu-Qin Dong*[a] and Chun-Jiang Wang*[ab]

The development of enantioselective annulation reactions using readily available substrates for the construction of structurally and stereochemically diverse heterocycles is a compelling topic in diversity-oriented synthesis. Herein, we report efficient catalytic asymmetric formal 1,3-dipolar (3 + 4) cycloadditions of azomethine ylides with 4-indolyl allylic carbonates for the construction of azepino[3,4,5-*cd*]-indoles fused with a challenging seven-membered N-heterocycle, a frequently occurring tricyclic indole scaffold in bioactive compounds and pharmaceuticals. Through cooperative Cu/Ir-catalyzed asymmetric allylic alkylation followed by intramolecular Friedel–Crafts reaction, an array of azepino[3,4,5-*cd*]-indoles were obtained in good yields with excellent diastereo-/enantioselective control. More importantly, the full stereodivergence of this transformation was established *via* synergistic catalysis followed by acid-promoted epimerization, and up to eight stereoisomers of the cycloadducts bearing three stereogenic centers could be predictably achieved from the same set of starting materials for the first time. Quantum mechanical computations established a plausible mechanism for the synergistic Cu/Ir catalysis to stereodivergently introduce two vicinal stereocenters whose stereochemical information is remotely delivered across the fused azepine ring to control the third chiral center. Epimerization of the last center involves protonation-enabled reversal of the thermodynamically controlled relative configuration.

Received 31st December 2021
Accepted 27th March 2022

DOI: 10.1039/d1sc07271d

rsc.li/chemical-science

Introduction

Transforming simple precursors into a library of natural product-like or drug-like scaffolds with skeletal and stereochemical diversity remains an important objective as well as a huge challenge in diversity-oriented synthesis (DOS).[1] As a straightforward methodology to serve such endeavors, the so-called reagent-based or branching DOS approach which involves the application of different reaction partners/conditions to access distinct molecular architectures from a common substrate has received considerable attention.[2] For example, the diversity-oriented synthesis of enantioenriched N-heterocycles using *in situ* generated azomethine ylides (AMYs) from readily available aldimine esters as key building blocks has been intensively studied for decades (Scheme 1a).[3,4] Specifically, transition-metal catalyzed asymmetric 1,3-dipolar (3 + 2) cycloadditions of AMYs with electron-deficient alkenes are known to be one of the most important tools for the construction of five-membered chiral pyrrolidines.[5] Recent developments in enantioselective higher order (3 + 3) cycloaddition further extended the synthetic applicability of AMYs to approach six-membered N-heterocycles including piperidines and 1,4,5-triazines.[6] In contrast, assembling important skeletons other than five-/six-membered rings, for instance, seven-membered N-heterocycles, *via* 1,3-dipolar (3 + 4) cycloaddition of AMYs is extremely difficult owing to the disfavored entropic factors and transannular interactions[7] and the challenge in stereocontrol of multiple stereogenic centers.[4] In 2014, we reported an Et_3N-catalyzed formal (3 + 4) annulation of aldimine esters with methyl coumalate for the preparation of functionalized racemic azepine derivatives.[8a] However, the catalytic asymmetric 1,3-dipolar (3 + 4) cycloaddition of AMYs, especially

[a]*Engineering Research Center of Organosilicon Compounds & Materials, Ministry of Education, College of Chemistry and Molecular Sciences, Wuhan University, Wuhan, 430072, China. E-mail: cjwang@whu.edu.cn; xiuqindong@whu.edu.cn*

[b]*State Key Laboratory of Elemento-organic Chemistry, Nankai University, Tianjin, 300071, China*

[c]*Tianjin Key Laboratory of Molecular Optoelectronic Sciences, Department of Chemistry, Tianjin University, Tianjin, 300072, China. E-mail: yanfeng.dang@tju.edu.cn*

† Electronic supplementary information (ESI) available. CCDC 2090369–2090371. For ESI and crystallographic data in CIF or other electronic format see DOI: 10.1039/d1sc07271d

‡ These two authors contributed equally.

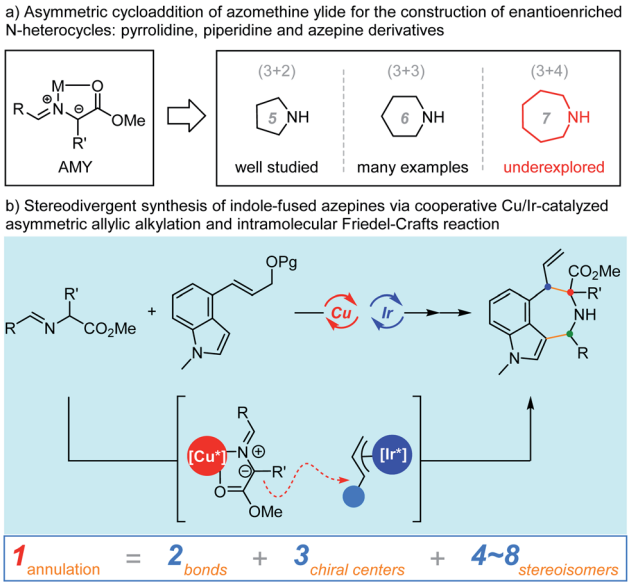

Scheme 1 Synthetic approaches to chiral azepino[3,4,5-*cd*]indoles.

for the construction of seven-membered N-heterocycles featuring stereodivergence, remains elusive and a formidable task.

On the other hand, the stereochemical diversity in cycloaddition reactions represents another challenging subject in organic synthesis. For bioactive compounds and pharmaceutical molecules bearing multiple stereogenic centers, both absolute and relative configurations can greatly affect their biological activities.[9] Therefore, the development of reliable and facile access to all stereoisomers of a relevant scaffold from the same starting materials would be highly significant. In recent years, the strategy of synergistic catalysis has attracted extensive attention in the area of stereodivergent synthesis,[10,11] which offers access to all four stereoisomeric compounds bearing two stereogenic centers through judicious permutation of two individual chiral catalysts, which simultaneously activate two different reaction partners, respectively.[12,13] Recently, such a strategy has been successfully applied in Cu/Ir-catalyzed stereodivergent 1,3-dipolar (3 + 3) cycloaddition of AMYs with 2-indolyl allyl carbonates, furnishing enantioenriched tetrahydro-γ-carbolines bearing three stereogenic centers with the stereoselective formation of only four isomers among the total eight stereoisomers.[14] Despite these achievements, to the best of our knowledge, catalytic stereodivergent 1,3-dipolar cycloaddition of AMYs for the precise construction of all eight stereoisomers of N-heterocycles incorporating three stereogenic centers is unprecedented. We anticipated that the ambiphilic π-allyl-iridium species *in situ* generated from 4-indolyl allylic carbonates may serve as a unique 4-atom unit in formal 1,3-dipolar (3 + 4) cycloaddition of azomethine ylides,[15] providing a novel route to azepino[3,4,5-*cd*] indole derivatives through asymmetric allylic alkylation[16] followed by intramolecular Friedel–Crafts reaction[17] (Scheme 1b). The chiral azepino[3,4,5-*cd*] indole framework is present in numerous bioactive compounds and pharmaceuticals,[18,19] while very few examples have been documented for its enantioselective preparation so far.[20] Herein, we report the development of cooperative Cu/Ir-catalyzed formal 1,3-dipolar (3 + 4) cycloaddition of azomethine ylides to afford azepino[3,4,5-*cd*]-indole derivatives bearing three stereogenic centers with high diastereo- and enantiocontrol. Importantly, combining synergistic catalysis and late-stage epimerization allows the precise construction of all eight stereoisomers of the 3,4-fused tricyclic indoles, thus making the current transformation fully stereodivergent.

Results and discussion

Condition optimization

To examine the feasibility of the designed azepino[3,4,5-*cd*]-indole synthesis, we first explored the reaction using alanine derived aldimine ester **1a** (serving as an AMY precursor) and (*E*)-4-indolyl allyl carbonate **2a** (serving as a π-allyl-Ir precursor) as the model substrates, and K_2CO_3 as the base in dichloroethane at room temperature. With the dual [Cu(I)/(*S*,*S*$_p$)-**L1** + Ir(I)/(*R*,*R*$_a$)-**L4**] catalyst combination utilized in our previous stereodivergent 1,3-dipolar (3 + 3) cycloaddition of AMYs with (*E*)-2-indolyl allyl carbonates,[14] unfortunately, no desired (3 + 4) cycloadduct **3a** was observed, while isolation of the reaction mixture indicated that the reaction was interrupted in the first coupling step. We envisioned that the addition of a stronger Lewis acid might be able to activate the imine moiety of the allylation intermediate and thus promote the subsequent intramolecular Friedel–Crafts reaction.[17] To our delight, 0.5 equivalents of $Zn(OTf)_2$ significantly accelerated the desired cyclization, furnishing the cycloadduct azepino[3,4,5-*cd*] indole 6,9-*cis*-**3a** in 52% yield with unsatisfactory diastereoselectivity (3 : 1 dr; only 6,9-*cis*-isomers were formed due to the subsequent cyclization step being stereospecific) albeit with excellent enantioselectivity (99% ee for both isomers) (Table 1, entry 1). To improve the diastereoselectivity control, chiral phosphoramidite ligands[21a] (**L5** and **L6**) commonly used in Ir-catalyzed asymmetric allylic alkylation were then evaluated for this reaction. With the combination of [Cu(I)/(*S*,*S*$_p$)-**L1** + Ir(I)/(*S*$_a$,*S*,*S*)-**L5**] as the dual catalysts, the sequential reaction proceeded smoothly to afford the desired cycloadduct in 55% yield with high diastereoselectivity (18 : 1 dr) and excellent enantioselectivity (99% ee) (Table 1, entry 2). Lower diastereoselectivity was observed when using bulky *ortho*-methoxy substituted phosphoramidite **L6** as the chiral ligand for the iridium complex (entry 3). Further screening of chiral Phosferrox ligands[21b] for the copper complex ((*S*,*S*$_p$)-**L1–L3**) and iridium complex ((*S*$_a$,*S*,*S*)-**L5** and (*S*$_a$,*S*,*S*)-**L6**) identified the combination of [Cu(I)/(*S*,*S*$_p$)-**L1** + Ir(I)/(*S*$_a$,*S*,*S*)-**L5**] as optimal in terms of diastereo-/enantioselectivity (entries 3–5). With the catalytic system established, we then examined various additives to improve the yield. Among the tested Lewis/Brønsted acids, zinc oxide[22] led to no reaction at all, while metal triflates such as $Sc(OTf)_3$, $Yb(OTf)_3$ and $Sn(OTf)_2$ afforded moderate yields with 9 : 1 to 17 : 1 dr (entries 6–9). Other promoters including $Et_2O\cdot BF_3$ and $(PhSO_2)_2NH$ gave no better results either (entries 10 and 11). Carefully monitoring the reaction by NMR experiments revealed that the unsatisfactory yield was mainly caused by the

Table 1 Optimization of reaction conditions[a]

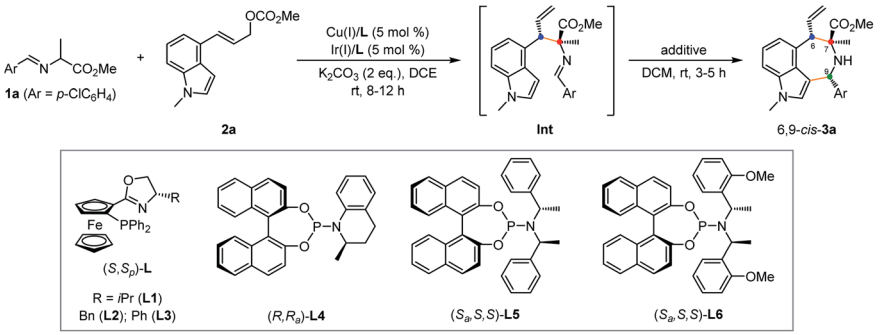

Entry	L for Cu(I)	L for Ir(I)	Additive (mol%)	dr[b]	Yield (%)[c]	ee (%)[d]
1	(S,S_p)-**L1**	(R,R_a)-**L4**	$Zn(OTf)_2$ (50)	3 : 1	52	99
2	(S,S_p)-**L1**	(S_a,S,S)-**L5**	$Zn(OTf)_2$ (50)	18 : 1	55	99
3	(S,S_p)-**L1**	(S_a,S,S)-**L6**	$Zn(OTf)_2$ (50)	12 : 1	58	99
4	(S,S_p)-**L2**	(S_a,S,S)-**L5**	$Zn(OTf)_2$ (50)	16 : 1	60	99
5	(S,S_p)-**L3**	(S_a,S,S)-**L5**	$Zn(OTf)_2$ (50)	14 : 1	54	99
6	(S,S_p)-**L1**	(S_a,S,S)-**L5**	ZnO (50)	—	—	—
7	(S,S_p)-**L1**	(S_a,S,S)-**L5**	$Sc(OTf)_3$ (50)	15 : 1	45	99
8	(S,S_p)-**L1**	(S_a,S,S)-**L5**	$Yb(OTf)_3$ (50)	17 : 1	55	99
9	(S,S_p)-**L1**	(S_a,S,S)-**L5**	$Sn(OTf)_2$ (50)	9 : 1	35	99
10	(S,S_p)-**L1**	(S_a,S,S)-**L5**	$(PhSO_2)_2NH$ (50)	14 : 1	57	99
11	(S,S_p)-**L1**	(S_a,S,S)-**L5**	$Et_2O\cdot BF_3$ (20)	4 : 1	40	99
12[e]	(S,S_p)-**L1**	(S_a,S,S)-**L5**	$Yb(OTf)_3$ (50)	16 : 1	65	99
13[e]	(S,S_p)-**L1**	(S_a,S,S)-**L5**	$Zn(OTf)_2$ (50)	18 : 1	67	99
14	(S,S_p)-**L1**	—	$Zn(OTf)_2$ (50)	—	—	—
15	—	(S_a,S,S)-**L5**	$Zn(OTf)_2$ (50)	—	—	—

[a] All reactions were carried out with 0.30 mmol **1a** and 0.20 mmol **2a** in 2 mL of DCE. Cu(I) = $Cu(MeCN)_4BF_4$. Ir(I) = $[Ir(cod)Cl]_2$. [b] dr was determined by the ^1H NMR of the crude reaction mixture. [c] Isolated yields of the overall two steps. [d] ee was determined by chiral HPLC analysis. [e] 2 equiv. of 4-chlorobenzaldehyde was added.

decomposition of an imine-containing allylation intermediate in the cyclization step, and no other byproduct was observed in this transformation. Accordingly, we examined the feasibility of adding an external aldehyde to minimize the undesired imine-decomposition with yield improvement although it is a limitation of this method. Gratifyingly, the cyclization proceeded smoothly in the presence of 0.5 equivalents of $Zn(OTf)_2$ and two equivalents of *p*-chlorobenzaldehyde, delivering **3a** in 67% yield with maintained diastereoselectivity and enantioselectivity (entry 13). (*Z*)-4-indolyl allyl carbonate **2a′** was not a viable reactant partner in this transformation due to the less efficiency of the allylation step. Additionally, both of copper and iridium catalysts are critical for the efficiency of the initial coupling reaction. Without either of these two metal complexes, no reaction occurred under otherwise identical reaction conditions (entries 14 and 15).

Substrate scope

With the optimal reaction conditions in hand, we set out to explore the substrate scope of azomethine ylide precursors in this cycloaddition. As illustrated in Table 2, an array of aromatic aldehyde derived imine esters **1** underwent efficient asymmetric allylic alkylation/intramolecular Friedel–Crafts reaction with **2a**, producing the corresponding azepino[3,4,5-*cd*]-indoles **3a–m** in moderate to good yields with high diastereoselectivities and excellent enantioselectivities (Table 2, entries 1–13). The substituents on the aryl ring of aldimine esters **1** with different electronic properties (electron-withdrawing, -neutral and -donating) in different positions (*para*-, *meta*- and *ortho*-) displayed a negligible influence on the stereochemical outcome. Heterocyclic 2-thienyl and 2-furyl aldimine esters exhibited comparable levels of reactivity, giving the desired cycloadducts **3n** and **3o** in synthetically acceptable yields with high diastereoselectivities and 99% ee (entries 14 and 15). In addition, the less reactive aliphatic aldehyde derived imine ester was tolerated well and the corresponding cycloadduct **3p** was isolated in moderate yield with excellent stereoselective control (entry 16). Moreover, the reaction of 2-amino-γ-butyrolactone derived aldimine ester **1q** with **2a** proceeded smoothly, affording the desired spiro heterocyclic azepino[3,4,5-*cd*] indole **3q** in 62% yield with good dr and 99% ee (entry 17). Next, azomethine ylides derived from various natural and unnatural amino acid esters were subjected to this reaction. Aldimine esters containing alkyl, allyl, ether or ester functional groups at the α-position all proved to be viable, furnishing the desired cycloadducts **3r–v** in acceptable yields with 19 : 1 to 20 : 1 dr and 99% ee (entries 18–22). No reaction occurred when an α-phenyl

Table 2 Substrate scope of aldimine esters[a]

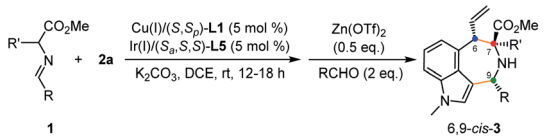

Entry	R	R'	3	dr[b]	Yield (%)[c]	ee (%)[d]
1	p-ClC_6H_4	Me	**3a**	18 : 1	67	99
2	p-BrC_6H_4	Me	**3b**	19 : 1	68	99
3	p-FC_6H_4	Me	**3c**	17 : 1	64	99
4	m-ClC_6H_4	Me	**3d**	14 : 1	62	99
5	m-BrC_6H_4	Me	**3e**	16 : 1	70	98
6	Ph	Me	**3f**	15 : 1	68	99
7	p-MeC_6H_4	Me	**3g**	12 : 1	60	97
8	p-$MeOC_6H_4$	Me	**3h**	18 : 1	66	99
9	m-MeC_6H_4	Me	**3i**	15 : 1	58	99
10	m-$MeOC_6H_4$	Me	**3j**	16 : 1	61	99
11	o-MeC_6H_4	Me	**3k**	11 : 1	63	99
12	o-ClC_6H_4	Me	**3l**	15 : 1	66	99
13	o-BrC_6H_4	Me	**3m**	15 : 1	64	99
14	2-thienyl	Me	**3n**	14 : 1	58	99
15	2-furyl	Me	**3o**	10 : 1	55	99
16	n-Pr	Me	**3p**	11 : 1	44	99
17	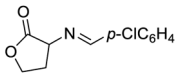		**3q**	10 : 1	62	99
18	p-ClC_6H_4	Et	**3r**	20 : 1	66	99
19	p-ClC_6H_4	n-Pr	**3s**	20 : 1	63	99
20[e]	p-ClC_6H_4	Allyl	**3t**	20 : 1	66	99
21	p-ClC_6H_4	$CH_2O$$t$-Bu	**3u**	20 : 1	65	99
22	p-ClC_6H_4	$CH_2CH_2CO_2Me$	**3v**	19 : 1	58	99
23	p-ClC_6H_4	H	**3w**	9 : 1	54	99
24[f]	p-ClC_6H_4	Me	**3a**	15 : 1	68	99

[a] All reactions were carried out with 0.30 mmol **1** and 0.20 mmol **2a** in 2 mL of DCE. Cu(I) = $Cu(MeCN)_4BF_4$. Ir(I) = $[Ir(cod)Cl]_2$. [b] dr was determined by the ^1H NMR of the crude reaction mixture. [c] Isolated yields of the overall two steps. [d] ee was determined by chiral HPLC analysis. [e] Ethyl aldimine ester. [f] 1.0 mmol scale.

substituted aldimine ester was employed probably due to the unfavourable steric hindrance. The current protocol could also be readily extended to a glycine derived azomethine ylide, which worked as a suitable partner to deliver the corresponding product **3w** with good diastereoselectivity (9 : 1 dr) and excellent enantioselectivity (99% ee, entry 23). Additionally, comparable diastereoselectivity and enantioselectivity were maintained in a 1.0 mmol (**2a**) scale reaction (entry 24).

Then, we turned our attention to examine the scope of 4-indolyl allyl carbonates and the results are summarized in Table 3. We were pleased to observe that indole moieties bearing halogen, phenyl, vinyl or cyclopropyl substituents at the 5-, 6- or 7-position were compatible with this reaction, delivering the highly functionalized azepino[3,4,5-*cd*] indoles **3x-D** in moderate to good yields, good to high diastereoselectivities and excellent enantioselectivities (Table 3, entries 1–7). *N*-Allyl- or *N*-benzyl-protected 4-indolyl allyl carbonates were well tolerated in this transformation to afford the corresponding cycloadducts **3E** and **3F**, respectively, in good yields with high diastereoselectivities and excellent enantioselectivities (entries 8 and 9). *N*-unprotected 4-indolyl allyl carbonate also underwent the current formal 1,3-dipolar [3 + 4] cycloaddition with **1a**, providing the desired product **3G** in 66% yield with 11 : 1 dr and 99% ee (entry 10).

Next, we examined the feasibility of the stereodivergent access to the stereoisomers of azepino[3,4,5-*cd*] indole derivatives. Six aldimine esters (**1a**, **1n** and **1t–w**) were chosen as the representative substrates to react with 4-indolyl allyl carbonate **2a** using different sets of Cu/Ir catalyst combinations. As shown in Table 4, in each case, with the pairwise combination of the dual system from the complete four sets of catalyst permutations Cu(I)/(R,R_p)-**L1** or Cu(I)/(S,S_p)-**L1** with Ir(I)/(R_a,R,R)-**L5** or Ir(I)/(S_a,S,S)-**L5**, four 6,9-*cis*-isomers of all eight stereoisomers, that is, (6*S*,7*S*,9*R*)-, (6*R*,7*S*,9*S*)-, (6*R*,7*R*,9*S*)-, and (6*S*,7*R*,9*R*)-**3**, were precisely constructed in good yields with high diastereoselectivities and excellent enantioselectivities.

Scale-up experiments and synthetic application

To demonstrate the practicality of this methodology, a scale-up synthesis of azepino[3,4,5-*cd*]-indole with catalyst combination

Table 3 Substrate scope of 4-indolyl allylic carbonates[a]

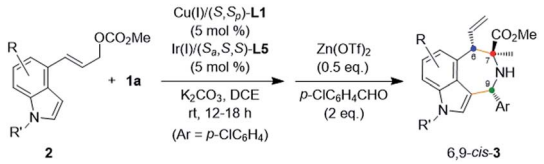

Entry	R	R'	3	dr[b]	Yield (%)[c]	ee (%)[d]
1	5-F	Me	**3x**	14 : 1	63	99
2	6-F	Me	**3y**	9 : 1	60	99
3	7-F	Me	**3z**	11 : 1	54	99
4	6-Br	Me	**3A**	12 : 1	63	99
5	6-Ph	Me	**3B**	20 : 1	56	99
6	6-vinyl	Me	**3C**	18 : 1	64	99
7	6-cyclopropyl	Me	**3D**	13 : 1	61	99
8	H	Allyl	**3E**	10 : 1	63	99
9	H	Bn	**3F**	15 : 1	61	97
10	H	H	**3G**	11 : 1	66	99

[a] All reactions were carried out with 0.30 mmol **1a** and 0.20 mmol **2** in 2 mL of DCE. Cu(I) = $Cu(MeCN)_4BF_4$. Ir(I) = $[Ir(cod)Cl]_2$. [b] dr was determined by the ^1H NMR of the crude reaction mixture. [c] Isolated yields of the overall two steps. [d] ee was determined by chiral HPLC analysis.

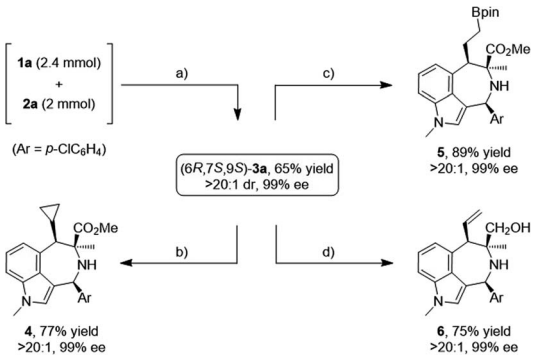

Scheme 2 Scale-up experiments and synthetic transformations.

[Cu(I)/(S,S_p)-**L1** + Ir(I)/(R_a,R,R)-**L5**] was performed under the optimal reaction conditions. To our delight, (6*R*,7*S*,9*S*)-**3a** could be obtained in good and comparable yield without loss of diastereoselective and enantioselective control (Scheme 2). Then, azepino[3,4,5-*cd*]-indole (6*R*,7*S*,9*S*)-**3a** obtained herein readily underwent different synthetic transformations. Palladium(II)-catalyzed cyclopropanation of (6*R*,7*S*,9*S*)-**3a** with diazomethane afforded the corresponding product **4** in a good yield with maintained diastereoselectivity and enantioselectivity.

Table 4 Representative examples of stereodivergence[a]

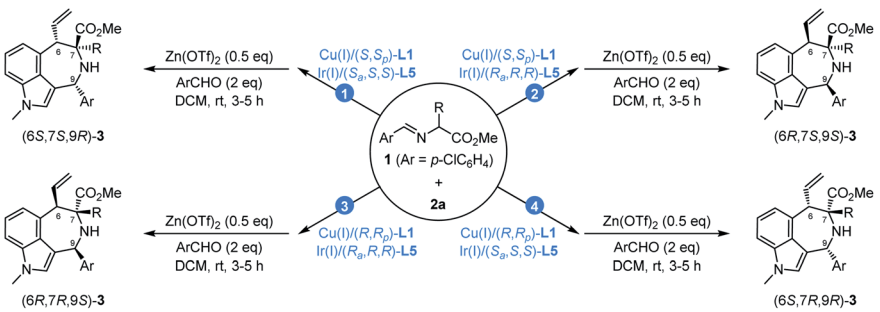

			Cooperative copper/iridium catalysts			
			Cu(I)/(S,S_p)-**L1**	Cu(I)/(S,S_p)-**L1**	Cu(I)/(R,R_p)-**L1**	Cu(I)/(R,R_p)-**L1**
entry	Ar	R	Ir/(S_a,S,S)-**L5**	Ir/(R_a,R,R)-**L5**	Ir/(R_a,R,R)-**L5**	Ir/(S_a,S,S)-**L5**
1	*p*-ClC_6H_4	Me	(6*S*,7*S*,9*R*)-**3a**, 67% yield 18 : 1 dr, 99% ee	(6*R*,7*S*,9*S*)-**3a**, 63% yield 20 : 1 dr, 99% ee	(6*R*,7*R*,9*S*)-**3a**, 62% yield 17 : 1 dr, 99% ee	(6*S*,7*R*,9*R*)-**3a**, 66% yield 20 : 1 dr, 99% ee
2[b]	2-thienyl	Me	(6*S*,7*S*,9*S*)-**3n**, 58% yield 14 : 1 dr, 99% ee	(6*R*,7*S*,9*R*)-**3n**, 45% yield 10 : 1 dr, 99% ee	(6*R*,7*R*,9*R*)-**3n**, 60% yield 14 : 1 dr, 99% ee	(6*S*,7*R*,9*S*)-**3n**, 52% yield 10 : 1 dr, 99% ee
3	*p*-ClC_6H_4	$CH_2CH{=}CH_2$	(6*S*,7*S*,9*R*)-**3t**, 66% yield 20 : 1 dr, 99% ee	(6*R*,7*S*,9*S*)-**3t**, 60% yield 20 : 1 dr, 99% ee	(6*R*,7*R*,9*S*)-**3t**, 60% yield 19 : 1 dr, 99% ee	(6*S*,7*R*,9*R*)-**3t**, 62% yield 20 : 1 dr, 99% ee
4[b]	*p*-ClC_6H_4	CH_2O*t*-Bu	(6*S*,7*R*,9*R*)-**3u**, 65% yield 20 : 1 dr, 99% ee	(6*R*,7*R*,9*S*)-**3u**, 60% yield 20 : 1 dr, 99% ee	(6*R*,7*S*,9*S*)-**3u**, 61% yield 20 : 1 dr, 99% ee	(6*S*,7*S*,9*R*)-**3u**, 62% yield 19 : 1 dr, 99% ee
5	*p*-ClC_6H_4	$(CH_2)_2CO_2Me$	(6*S*,7*S*,9*R*)-**3v**, 58% yield 20 : 1 dr, 99% ee	(6*R*,7*S*,9*S*)-**3v**, 54% yield 20 : 1 dr, 99% ee	(6*R*,7*R*,9*S*)-**3v**, 52% yield 19 : 1 dr, 99% ee	(6*S*,7*R*,9*R*)-**3v**, 55% yield 18 : 1 dr, 97% ee
6	*p*-ClC_6H_4	H	(6*S*,7*S*,9*R*)-**3w**, 54% yield 9 : 1 dr, 99% ee	(6*R*,7*S*,9*S*)-**3w**, 52% yield 10 : 1 dr, 99% ee	(6*R*,7*R*,9*S*)-**3w**, 55% yield 10 : 1 dr, 99% ee	(6*S*,7*R*,9*R*)-**3w**, 56% yield 10 : 1 dr, 99% ee

[a] All reactions were carried out with 0.30 mmol **1** and 0.20 mmol **2a** in 2 mL of DCE within 12–18 h for allylation step. dr was determined by the ^1H NMR of the crude reaction mixture. Isolated yields of the overall two steps. ee was determined by chiral HPLC analysis. [b] Discrepancy in configuration is caused by the sequence rule.

Iridium(I)-catalyzed hydroboration of the terminal alkene in (6*R*,7*S*,9*S*)-**3a** delivered the *anti*-Markovnikov product **5** in 89% yield without loss of enantiopurity. Ester reduction with $NaBH_4$ provided the corresponding compound **6** in 75% yield with the retention of diastereoselectivity and enantioselectivity.

Exploration of stereodivergent synthesis of all eight stereoisomers

Based on the experimental results and X-ray diffraction analysis of the achieved cycloadducts (*vide infra*),[23] we postulated that the stereochemical outcome of this formal 1,3-dioplar (3 + 4) cycloaddition originated from a cooperative Cu/Ir-catalyzed stereodivergent asymmetric allylic alkylation followed by a stereospecific intramolecular Friedel–Crafts reaction, thus only four 6,9-*cis*-isomers of all eight stereoisomers could be prepared with the distinct permutations of the four sets of chiral Cu and chiral Ir catalysts. C9-epimerization of the 6,9-*cis*-isomers would be an ideal pathway for expedient access to the other four stereoisomers (6,9-*trans*-isomers). All C9-epimerization attempts failed under basic conditions.[24] However, to our delight, C9-epimerization of the 6,9-*cis*-cycloadducts could be readily realized through the TFA-promoted ring-opening-cyclization reaction. In the presence of 2 equivalents of trifluoroacetic acid (TFA) in dichloromethane, 6,9-*cis*-isomers (6*S*,7*S*,9*R*)-**3a** and (6*R*,7*R*,9*S*)-**3a** could be efficiently converted into the corresponding 6,9-*trans*-isomers (6*S*,7*S*,9*S*)-**3a** and (6*R*,7*R*,9*R*)-**3a**, respectively, without any erosion of enantioselectivity (Scheme 3A). Additionally, (6*S*,7*S*,9*S*)-**3a** and (6*R*,7*R*,9*R*)-**3a** could be directly achieved through a one-pot allylation/cyclization/epimerization process when using TFA as the cyclization promoter (see the ESI† for details). Less efficient C9-epimerization was observed for the other two 6,9-*cis*-isomers (6*R*,7*S*,9*S*)-**3a** and (6*S*,7*R*,9*R*)-**3a**, and moderate yields of the corresponding enantioenriched 6,9-*trans*-isomers (6*R*,7*S*,9*R*)-**3a** and (6*S*,7*R*,9*S*)-**3a** were obtained with the 6,9-*cis*-isomers being recovered. Nevertheless, the chemical yields of the two 6,9-*trans*-stereoisomers could be readily improved through iteration of TFA-promoted C9-epimerization (Scheme 3B). The absolute configurations of the cycloadduct (6*S*,7*S*,9*R*)-**3a** and the two epimerized (6*R*,7*R*,9*R*)-**3a** and (6*R*,7*S*,9*R*)-**3a** were unequivocally determined by X-ray diffraction analysis.[23]

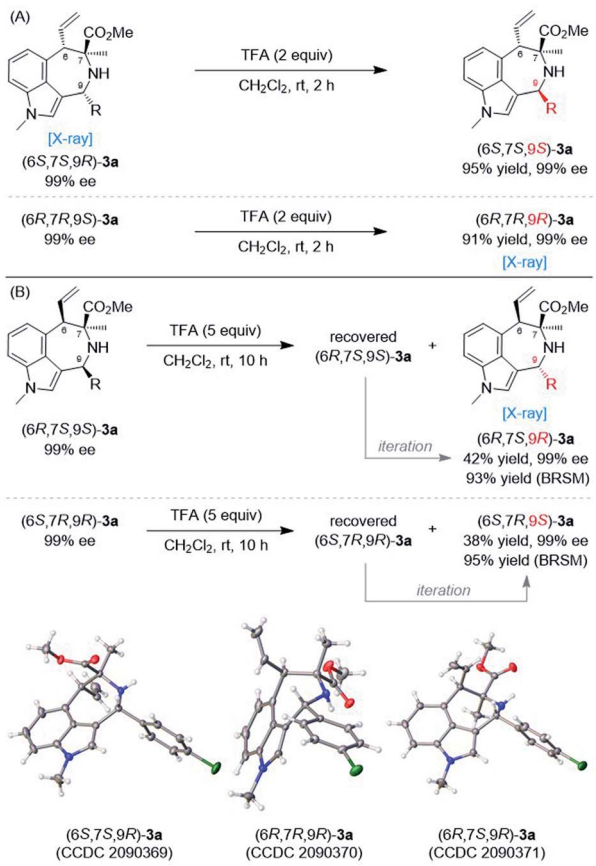

Scheme 3 TFA-promoted C9-epimerization of 6,9-*cis*-**3a** to access another four 6,9-*trans*-**3a** stereoisomers.

Computational mechanistic studies

Using quantum mechanical computations,[25] we investigated the mechanism by which the azepino[3,4,5-*cd*]-indole products are stereoselectively constructed with generation of three chiral centers. The M06-L functional[26] was used on account of the balanced performance for main-group and transition-metal chemistry and the ability to describe non-covalent interactions. Notably, the mechanism involves an array of stereocontrolling steps that dictate the absolute configurations at the C6/C7/C9 sites, respectively. Initial stereochemical information is introduced by synergistic Cu/Ir catalysis at the C6/C7 positions in the enantio- and diastereodivergent formation of the C6–C7 bond to rapidly build up molecular complexity. This dual-catalytic process will be studied first.[27,28] The ensuing steps feature achiral reagent promoted cyclization and epimerization with effective delivery of chirality, which will be explored later.

a. Synergistic Cu/Ir catalysis. In light of the stereospecific *anti*-attack on the allyl-iridium in the C6–C7 bond-forming step, we reasoned that the absolute configuration at C6 is determined by the stereochemical structure of π-allyl-iridium species, which is formed from the oxidative addition of 4-indolyl allyl carbonate **2a** with Ir(I) (see Fig. 1A for the schematic description and Fig. 1B for the computations). We considered an activated form of the iridium catalyst **IM1**, which contains a metallacyclic structure with the ligations of **L5** and COD.[29] In the presence of (*S*,*S*,*S*)-**L5**, the competition of **TS1a** *vs.* **TS1b** exhibits a large barrier difference of 2.9 kcal mol^{-1}, favoring the formation of π-allyl-iridium **IM3a**. Meanwhile, **IM3a** is 2.9 kcal mol^{-1} lower in free energy than the diastereomeric **IM3b**. The kinetic and thermodynamic preference for **IM3a** led us to infer that it represents the predominant allyl-iridium whereby the C6 stereocenter can be furnished through the *anti*-displacement-type coupling with the nucleophilic Cu-AMY species **IM4**. The computations allow us to correctly predict a 6*S* stereocenter when applying (*S*,*S*,*S*)-**L5** (and 6*R* with (*R*,*R*,*R*)-**L5**).

In attempts to understand the stereodiscrimination of allyl-iridium governing C6 stereochemistry, we explored how the chiral Ir catalyst creates the observed energetic differences in

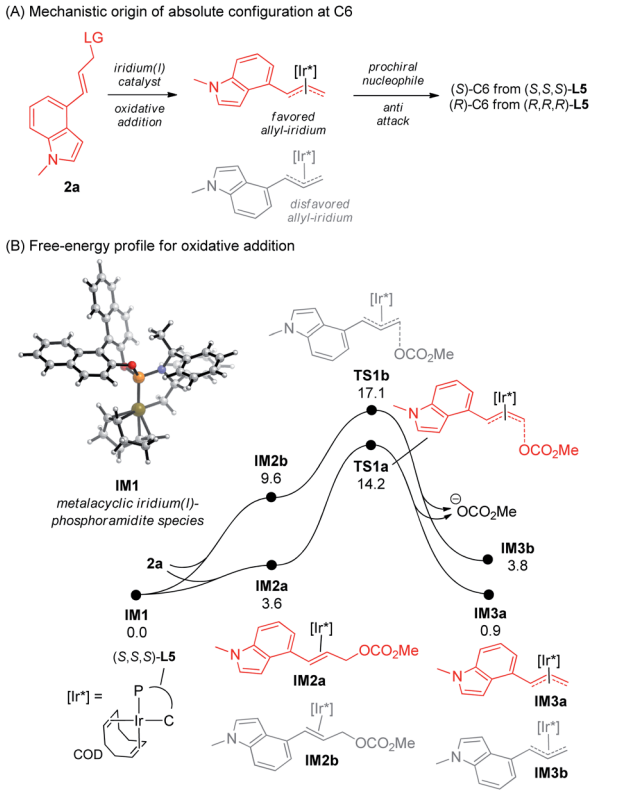

Fig. 1 Mechanistic origin of C6 stereoselectivity. Oxidative addition of **2a** with the activated iridium catalyst. Free energies are provided in kcal mol^{-1}.[30]

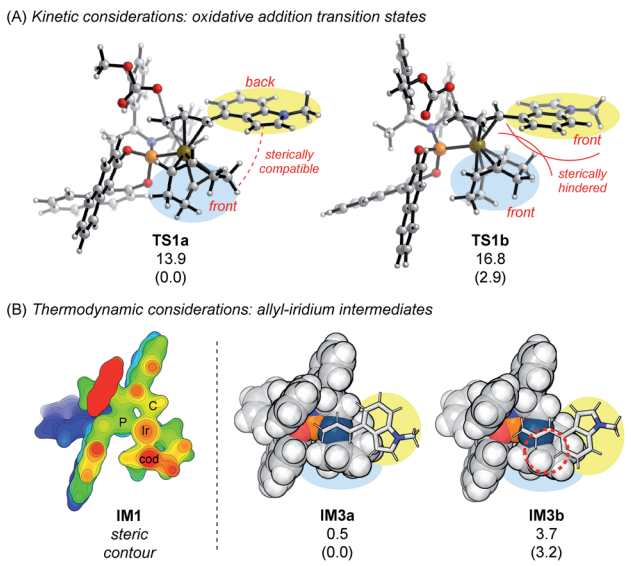

Fig. 2 Steric analysis for C6 stereoselectivity. Free energies are provided in kcal mol^{-1}, with relative values in parentheses.[31,32]

TS1 and **IM3**. For the former, we notice, as visualized in Fig. 2A, that the steric bulk of COD (blue, front) is circumvented by the indolyl unit (yellow, back) in **TS1a**, while the same structures result in a steric impediment to the catalyst–substrate interactions in **TS1b**. Such features have been carried over to allyl-iridium **IM3a**/**IM3b** to cause stronger steric repulsions in the latter, which is described in Fig. 2B. The comparisons reflect the effectiveness of the Ir catalyst in selectively exposing one π-allyl diastereoface for the following transformations.

With an understanding of the generation of allyl-iridium, we investigated the coupling of the electrophilic allyl-iridium **IM3a** with the nucleophilic Cu-AMY complex **IM4** to rationalize the stereoselectivity for the C7 center.[27,28] The mechanistic origin of the C7-stereoselection lies in a diastereofacial preference of the AMY unit (Fig. 3A). Despite simultaneous engagement of two chiral catalysts in the coupling step, Table 4 indicates that the stereochemical outcome at C7 depends exclusively on **L1**. To reveal the underlying mode of stereoinduction, the combinations of (*S*,*S*)-**L1** with (*S*,*S*,*S*)-**L5** (**TS2**/**TS2'**) and (*R*,*R*,*R*)-**L5** (**TS3**/**TS3′**) were studied. Regarding the Ir catalyst, it follows from previous analysis that (*S*,*S*,*S*)-**L5** and (*R*,*R*,*R*)-**L5** will selectively give **IM3a** and its enantiomer ***ent*-IM3a**, respectively. For the Cu catalyst, evaluation of the two possible diastereomers of the Cu-AMY complex discloses smaller steric repulsions when the aryl group is arranged on the unoccupied side of **L1**, leading to a free-energy difference of 2.6 kcal mol^{-1} favoring the participation of **IM4**, the main form of Cu-AMY, in C6–C7 coupling (see Fig. S1 in the ESI† for details). On the basis of these considerations, the transition states for the interception of allyl-iridium **IM3a**/***ent*-IM3a** by Cu-AMY species **IM4** were calculated (Fig. 3B). For both catalyst combinations, stereoregulation by (*S*,*S*)-**L1** makes the *si* face of the AMY moiety more favorable than the *re* face, regardless of the absolute configuration of **L5**, thus generating a 7*S* stereocenter. The notable barrier differences (4.7 and 6.4 kcal mol^{-1}) contribute to the excellent ee, and the correspondence between (*S*,*S*)-**L1** and 7*S* agrees with experiments.

The three-dimensional transition-state structures on display in Fig. 3B indicate a shared mode of stereoinduction for the two catalyst combinations. The *si*-TSs **TS2**/**TS3** not only manifest good structural matching between the catalyst-bound activated substrates but also involve C–H···π interactions of COD and the indolyl group with the –PPh_2 phosphino moiety of **L1** (see Fig. S2 in the ESI† for a visual analysis of non-covalent interactions). The *re*-TSs, in contrast, are disfavored because an *i*-Pr group on **L1** presents a steric obstacle to the approaching allyl-iridium. As supported by a further structural analysis in Fig. 3C, while the relative orientations of the two reactive species are controlled by the steric bulk of **L5**, it is the stereocontrol elements of **L1** that act as the main origin of AMY-diastereofacial selectivity. The **L1**-dependence of the resultant C7-stereoselectivity can be interpreted accordingly.

b. Zn(II)-promoted intramolecular Friedel–Crafts reaction. Having rationalized the generation of C6/C7 stereocenters by Cu/Ir synergistic catalysis, we sought to establish the mechanism of chirality transfer from existing stereocenters to C9 when treated by an achiral Lewis acid $Zn(OTf)_2$ (Fig. 4A). Notably, a strong stereochemical correlation between the C6 and C9 centers can be inferred from Table 4, *i.e.*, the formation of 9*R*/9*S* is apparently dictated by the initially introduced 6*S*/6*R* respectively to yield the 6,9-*cis*-isomers, while the configuration of C7 appears to be irrelevant. To gain a mechanistic

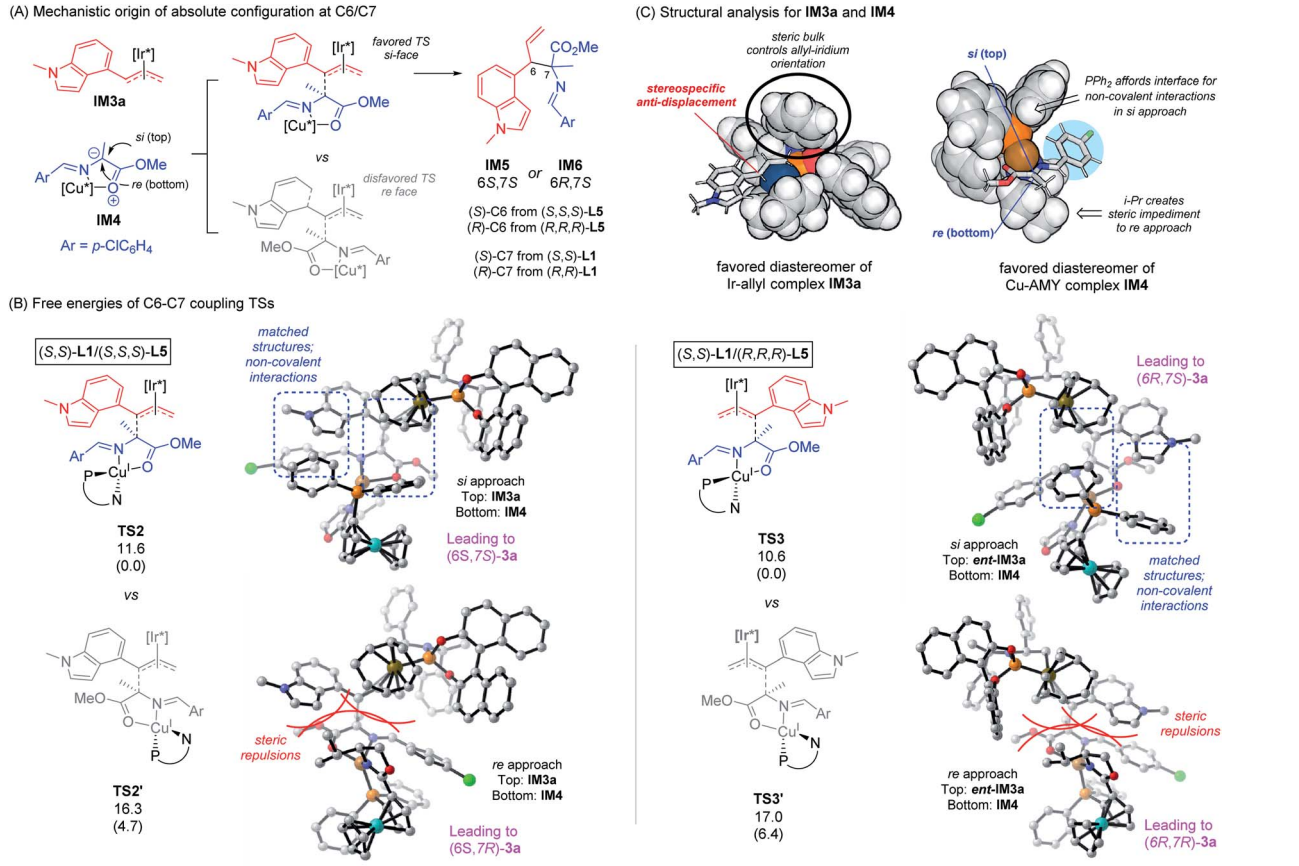

Fig. 3 Mechanistic origin of C7 stereoselectivity. Coupling between *in situ*-generated Cu-AMY species and π-allyl-iridium species. **IM3a**/**IM4** are used as energy zero. Free energies are provided in kcal mol^{-1}.

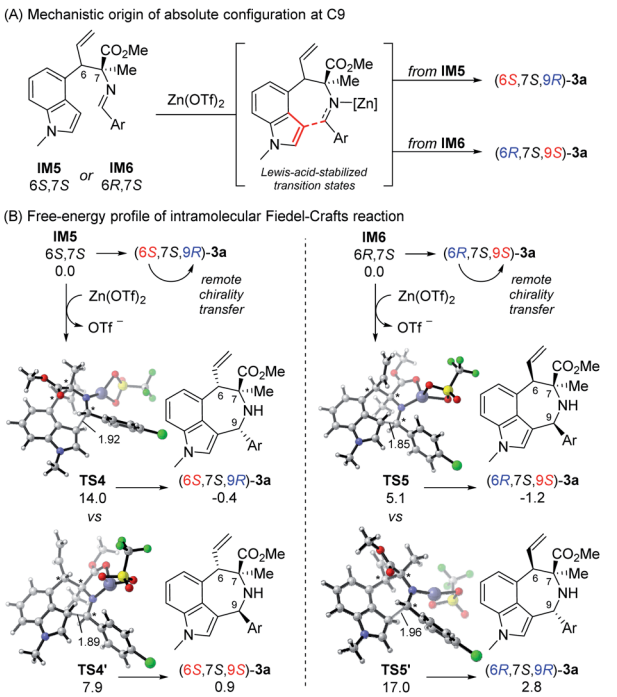

Fig. 4 Mechanistic origin of C9 stereoselectivity in Lewis-acid-promoted intramolecular Friedel–Crafts reaction. Free energies are provided in kcal mol^{-1} and distances in Å.

understanding, we hypothesize that the coordination of the Zn(II) Lewis acid on the allylation intermediate **IM5**/**IM6** can activate the electrophilic C=N bond and thus promote the cyclization to construct the desired azepino[3,4,5-*cd*]-indole skeleton.[33] Possible cyclization TSs were calculated and are presented in Fig. 4B. Interestingly, the assumption that the selectivity is kinetically controlled would lead to an incorrect stereochemical prediction for the cyclization of **IM5**, since **TS4**′ (yielding (6*S*,7*S*,9*S*)-**3a**) is lower in energy than **TS4** (yielding the observed (6*S*,7*S*,9*R*)-**3a**). Given the low barriers of **TS4**/**TS4**′, we speculated for **IM5** that a thermodynamic control of C9-stereoselectivity might be operative. The postulate is supported by the lower energy of (6*S*,7*S*,9*R*)-**3a** than the C9-epimer, the difference being 1.3 kcal mol^{-1}. With regard to **IM6**, (6*R*,7*S*,9*S*)-**3a** is calculated to be both the kinetic (**TS5** *vs.* **TS5**′) and the thermodynamic product, thus its formation can be unambiguously predicted from the computations.

c. TFA-promoted C9-Epimerization. Lastly, we turn to elucidate the mechanism of TFA-promoted C9-epimerization. We have found through studying Lewis-acid-enabled intramolecular Friedel–Crafts reaction that the combinations of 6*S*,9*R* and 6*R*,9*S* configurations result in higher thermodynamic stabilities than 6*S*,9*S* and 6*R*,9*R*, respectively, in the ring system. We thus investigated the driving force behind the C9-epimerization. For a possible explanation, the strong Brønsted

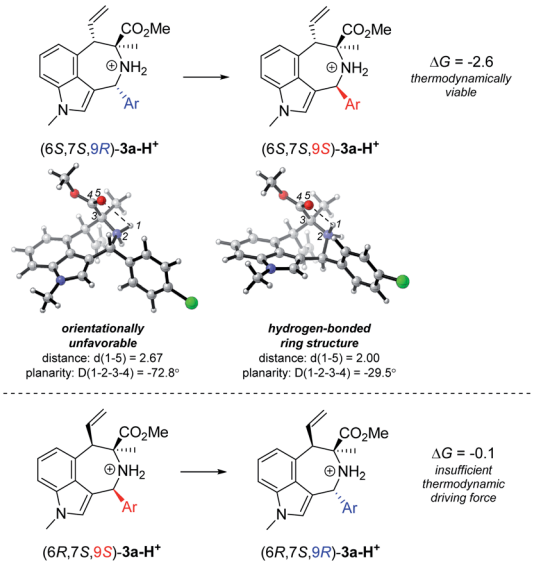

Fig. 5 Thermodynamics of TFA-promoted C9-epimerization. Free energies are in kcal mol^{-1} and distances in Å.

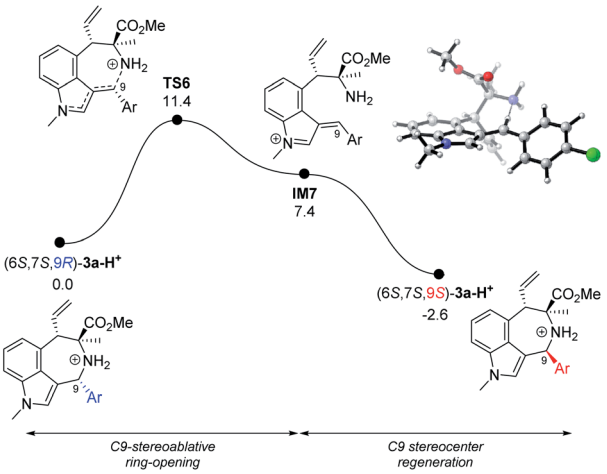

Fig. 6 Mechanism of TFA-promoted C9-epimerization for (6*S*,6*S*,9*R*)-**3a**. Free energies are provided in kcal mol^{-1}.

acid TFA might have protonated **3a** to reverse the epimerization thermodynamics and thus permit the transformation. Indeed, it can be seen from Fig. 5 that the C9-epimerization of the protonated (6*S*,7*S*,9*R*)-**3a-H**$^+$ is exergonic by −2.6 kcal mol^{-1}, suggesting adequate spontaneity. This is in contrast to the stability of (6*S*,7*S*,9*R*)-**3a** (see left in Fig. 4B) and can be ascribed to an intramolecular N–H···O hydrogen bond in the epimerized (6*S*,7*S*,9*S*)-**3a-H**$^+$ (see the 3D structures in Fig. 5). On the other hand, the free-energy change for the C9-epimerization of (6*R*,7*S*,9*S*)-**3a-H**$^+$ is only −0.1 kcal mol^{-1}, and equilibration with its C9-epimer is expected given sufficient time. The lack of driving force is partly because of the higher energy of the parent (6*R*,7*S*,9*R*)-**3a** which is 4.0 kcal mol^{-1} less stable than the epimeric (6*R*,7*S*,9*S*)-**3a** (see right in Fig. 4B). Upon comparing the predicted behaviors of **3a-H**$^+$ with the experimental results in Scheme 3, the obvious difference in yields and the amount of TFA can be very well explained, which in turn validates the computational models.

With the thermodynamics established, we calculated the free-energy profile in more detail to further our understanding of the mechanistic role of TFA. We envisioned that the acidic conditions might render **3a** prone to C9-stereoablation through a ring-opening C–N bond cleavage, followed by an aza-Michael reaction that re-constructs the ring with an opposite absolute configuration at the C9 center to yield the epimer. The proposed isomerization mechanism of (6*S*,7*S*,9*R*)-**3a** is shown in Fig. 6 (a similar profile is established for (6*R*,7*S*,9*S*)-**3a** and is provided in Fig. S3†). With a relatively low total barrier of 11.4 kcal mol^{-1} and intermediate energy of 7.4 kcal mol^{-1}, the proposed pathway can equilibrate the mixture in a reasonable amount of time to complete the C9-epimerization.

In summary, we have disclosed by quantum mechanical calculations that the stereodivergent construction of azepino [3,4,5]-indoles involves initial generation of vicinal C6/C7 stereocenters *via* cooperative Cu/Ir catalysis, which is followed by intramolecular Friedel–Crafts reaction with remote site-to-site chirality transfer from C6 to C9 assisted by an achiral Lewis acid. Subsequent treatment by a strong Brønsted acid can steer a late-stage C9-epimerization with a protonation-tuned thermodynamic tendency, stereoablative ring-opening and stereocenter regeneration *via* a second cyclization.

Conclusions

In conclusion, we have developed a cooperative Cu/Ir-catalyzed asymmetric allylic alkylation/intramolecular Friedel–Crafts reaction of azomethine ylides with 4-indolyl allyl carbonates, affording a facile access to a variety of biologically important chiral azepino[3,4,5-*cd*] indoles in a stereodivergent manner. The Cu-stabilized azomethine ylide *in situ* generated from aldimine esters serving as an ambiphilic 3-atom component and the unique π-allyl-iridium species *in situ* generated from 4-indolyl allylic carbonates serving as an ambiphilic 4-atom component were essential for the success of this stereodivergent formal 1,3-dipolar (3 + 4) cycloaddition of azomethine ylides. From the same set of starting materials, four 6,9-*cis*-stereoisomers of the cycloadduct could be accessed at will with excellent diastereoselectivity and enantioselectivity by employing an appropriate permutation of chiral copper and chiral iridium catalysts. Of particular note, merging the synergistic catalysis with TFA-promoted C9-epimerization enables the predictable preparation of all eight stereoisomers of the azepino [3,4,5-*cd*] indole derivatives bearing three stereogenic centers, which provides the first example of fully stereodivergent formal 1,3-dipolar (3 + 4) cycloaddition for the construction of seven-membered N-heterocycles. By quantum mechanical computations, we unravelled that the stereochemical information at the three stereocenters is sequentially established as the reaction proceeds, the key stereocontrolling steps being the generation of allyl-iridium, the diastereoface-selective coupling with Cu-AMY species, and the Lewis-acid-promoted intramolecular Friedel–Crafts reaction of the resultant allylation intermediate. The presence of a strong Brønsted acid can reverse the intrinsic

thermodynamic favorability of 6,9-*cis*-stereoisomers, reinstitute the allylated intermediate, and reconstruct the ring system with a 6,9-*trans*-stereoselectivity to complete the C9-epimerization, thus granting access to up to eight stereoisomers.

Data availability

All experimental and characterization data in this manuscript are available in the ESI.† Crystallographic data for compounds (6*S*,7*S*,9*R*)-**3a**, (6*R*,7*R*,9*R*)-**3a**, and (6*R*,7*S*,9*R*)-**3a** have been deposited at the CCDC and assigned numbers 2090369–2090371, respectively.

Author contributions

C. J. W. conceived and designed the research. C. J. W. and X. Q. D. directed the project. L. X., F. X. and C. F. performed the research. B. L. and Y. D. performed the DFT calculations. L. W., Y. D., and C. J. W. co-wrote the paper with assistance from L. X. and X. Q. D. All authors analyzed the data, discussed the results, and commented on the manuscript.

Conflicts of interest

There are no conflicts to declare.

Acknowledgements

This work was supported by NSFC (220711186, 220711187, and 22073067) and the Hubei Province Natural Science Foundation (2020CFA036 and 2021CFA069). The Program of Introducing Talents of Discipline to Universities of China (111 Project) is also appreciated.

Notes and references

1 S. L. Schreiber, *Science*, 2000, **287**, 1964–1969.

2 M. D. Burke and S. L. Schreiber, *Angew. Chem., Int. Ed.*, 2004, **43**, 46–58.

3 (*a*) C. Chen, X. Li and S. L. Schreiber, *J. Am. Chem. Soc.*, 2003, **125**, 10174–10175; (*b*) R. Huisgen, *Angew. Chem., Int. Ed.*, 1963, **2**, 565–598; (*c*) A. Padwa and W. H. Pearson, *Synthetic Applications of 1,3-Dipolar Cycloaddition Chemistry Toward Heterocycles and Natural Products*, Wiley-VCH, New York, 2002.

4 (*a*) L. Wei, X. Chang and C.-J. Wang, *Acc. Chem. Res.*, 2020, **53**, 1084–1100; (*b*) X. Fang and C. J. Wang, *Org. Biomol. Chem.*, 2018, **16**, 2591–2601; (*c*) J. Adrio and J. C. Carretero, *Chem. Commun.*, 2019, **55**, 11979–11991; (*d*) T. Hashimoto and K. Maruoka, *Chem. Rev.*, 2015, **115**, 5366–5412.

5 For the most recent examples of transition-metal catalyzed asymmetric 1,3-dipolar (3 + 2) cycloadditions, see: (*a*) X. Chang, Y. Yang, C. Shen, K.-S. Xue, Z.-F. Wang, H. Cong, H.-Y. Tao, L. W. Chung and C.-J. Wang, *J. Am. Chem. Soc.*, 2021, **143**, 3519–3535; (*b*) Z. Wang, D.-C. Wang, M.-S. Xie, G.-R. Qu and H.-M. Guo, *Org. Lett.*, 2020, **22**, 164–167; (*c*) H. Cui, K. Li, Y. Wang, M. Song, C. Wang, D. Wei, E.-Q. Li, Z. Duan and F. Mathey, *Org. Biomol. Chem.*, 2020, **18**, 3740–3746; (*d*) X. Cheng, D. Yan, X.-Q. Dong and C.-J. Wang, *Asian J. Org. Chem.*, 2020, **9**, 1567–1570; (*e*) X.-J. Zou, W.-L. Yang, J.-Y. Zhu and W.-P. Deng, *Chin. J. Chem.*, 2020, **38**, 435–438; (*f*) B. Liu, W. Li, H.-H. Wu and J. Zhang, *Org. Chem. Front.*, 2019, **6**, 694–698; (*g*) L. Liang, H.-Y. Niu, D.-C. Wang, X.-H. Yang, G.-R. Qu and H.-M. Guo, *Chem. Commun.*, 2019, **55**, 553–556; (*h*) Z. Gan, M. Zhi, R. Han, E.-Q. Li, Z. Duan and F. Mathey, *Org. Lett.*, 2019, **21**, 2782–2785; (*i*) X. Chang, X.-S. Sun, C. Che, Y.-Z. Hu, H.-Y. Tao and C.-J. Wang, *Org. Lett.*, 2019, **21**, 1191–1196; (*j*) G. S. Caleffi, O. Larranaga, M. Ferrandiz-Saperas, P. R. R. Costa, C. Najera, A. de Cozar, F. P. Cossio and J. M. Sansano, *J. Org. Chem.*, 2019, **84**, 10593–10605; (*k*) Y.-P. Zhang, Y. You, J.-Q. Zhao, X.-J. Zhou, X.-M. Zhang, X.-Y. Xu and W.-C. Yuan, *Org. Chem. Front.*, 2019, **6**, 1879–1884; (*l*) C. Shen, Y. Yang, L. Wei, W.-W. Dong, L. W. Chung and C.-J. Wang, *iScience*, 2019, **11**, 146–159; (*m*) F. Cheng, S. J. Kalita, Z.-N. Zhao, X. Yang, Y. Zhao, U. Schneider, N. Shibata and Y.-Y. Huang, *Angew. Chem., Int. Ed.*, 2019, **58**, 16637–16643; (*n*) Y. Xiong, Z. Du, H. Chen, Z. Yang, Q. Tan, C. Zhang, L. Zhu, Y. Lan and M. Zhang, *J. Am. Chem. Soc.*, 2019, **141**, 961–971.

6 For examples of transition-metal catalyzed asymmetric 1,3-dipolar (3 + 3) cycloadditions, see: (*a*) M.-C. Tong, X. Chen, H.-Y. Tao and C.-J. Wang, *Angew. Chem., Int. Ed.*, 2013, **52**, 12377–12380; (*b*) H. Guo, H. Liu, F.-L. Zhu, R. Na, H. Jiang, Y. Wu, L. Zhang, Z. Li, H. Yu, B. Wang, Y. Xiao, X.-P. Hu and M. Wang, *Angew. Chem., Int. Ed.*, 2013, **52**, 12641–12645; (*c*) C. Yuan, H. Liu, Z. Gao, L. Zhou, Y. Feng, Y. Xiao and H. Guo, *Org. Lett.*, 2015, **17**, 26–29; (*d*) W.-L. Yang, C.-Y. Li, W.-J. Qin, F.-F. Tang, X. Yu and W.-P. Deng, *ACS Catal.*, 2016, **6**, 5685–5690; (*e*) F. Xiao, S.-M. Xu, X.-Q. Dong and C.-J. Wang, *Org. Lett.*, 2021, **23**, 706–710; (*f*) M. Potowski, J. O. Bauer, C. Strohmann, A. P. Antonchick and H. Waldmann, *Angew. Chem., Int. Ed.*, 2012, **51**, 9512–9516; (*g*) Z.-L. He, H.-L. Teng and C.-J. Wang, *Angew. Chem., Int. Ed.*, 2013, **52**, 2934–2938; (*h*) Q.-H. Li, L. Wei and C.-J. Wang, *J. Am. Chem. Soc.*, 2014, **136**, 8685–8692; (*i*) H. Liu, Y. Wu, Y. Zhao, Z. Li, L. Zhang, W. Yang, H. Jiang, C. Jing, H. Yu, B. Wang, Y. Xiao and H. Guo, *J. Am. Chem. Soc.*, 2014, **136**, 2625–2629; (*j*) H.-L. Teng, L. Yao and C.-J. Wang, *J. Am. Chem. Soc.*, 2014, **136**, 4075–4080; (*k*) Z.-L. He, F. K. Sheong, Q.-H. Li, Z. Lin and C.-J. Wang, *Org. Lett.*, 2015, **17**, 1365–1368.

7 (*a*) G. A. Molander, *Acc. Chem. Res.*, 1998, **31**, 603–609; (*b*) C. Galli and L. Mandolini, *Eur. J. Org. Chem.*, 2000, 3117–3125.

8 (*a*) K. Liu, H.-L. Teng and C.-J. Wang, *Org. Lett.*, 2014, **16**, 4508–4511; (*b*) Z. Dai, J. Zhu, J. Wang, W. Su, F. Yang and Q. Zhou, *Adv. Synth. Catal.*, 2020, **362**, 545–551; (*c*) N. De and E. J. Yoo, Recent Advances in the Catalytic Cycloaddition of 1,*n*-Dipoles, *ACS Catal.*, 2018, **8**, 48–58.

9 (*a*) B. Waldeck, *Chirality*, 1993, **5**, 350–355; (*b*) F. Lovering, J. Bikker and C. Humblet, *J. Med. Chem.*, 2009, **52**, 6752–6756; (*c*) K. M. Rentsch, *J. Biochem. Biophys. Methods*, 2002, **54**, 1–9.

10 S. Krautwald, D. Sarlah, M. A. Schafroth and E. M. Carreira, *Science*, 2013, **340**, 1065–1068.

11 For selected reviews and perspectives on dual-metal catalysis, see:(*a*) S. Krautwald and E. M. Carreira, *J. Am. Chem. Soc.*, 2017, **139**, 5627–5639; (*b*) L. Lin and X. Feng, *Chem. – Eur. J.*, 2017, **23**, 6464–6482; (*c*) I. P. Beletskaya, C. Nájera and M. Yus, *Chem. Rev.*, 2018, **118**, 5080–5200; (*d*) Y. Wu, X. Huo and W. Zhang, *Chem. – Eur. J.*, 2020, **26**, 4895–4916; (*e*) U. B. Kim, D. J. Jung, H. J. Jeon, K. Rathwell and S.-g. Lee, *Chem. Rev.*, 2020, **120**, 13382–13433; (*f*) L. Wei and C.-J. Wang, *Chin. J. Chem.*, 2021, **39**, 15–24.

12 For selected representative stereodivergent synthesis using dual metal catalysts, metal/organocatalysts or dual organocatalysts, see: (*a*) S. Krautwald, M. A. Schafroth, D. Sarlah and E. M. Carreira, *J. Am. Chem. Soc.*, 2014, **136**, 3020–3023; (*b*) T. Sandmeier, S. Krautwald, H. F. Zipfel and E. M. Carreira, *Angew. Chem., Int. Ed.*, 2015, **54**, 14363–14367; (*c*) F. A. Cruz and V. M. Dong, *J. Am. Chem. Soc.*, 2017, **139**, 1029–1032; (*d*) X. Jiang, J. J. Beiger and J. F. Hartwig, *J. Am. Chem. Soc.*, 2017, **139**, 87–90; (*e*) X. Huo, R. He, X. Zhang and W. Zhang, *J. Am. Chem. Soc.*, 2016, **138**, 11093–11096; (*f*) X. Huo, R. He, J. Fu, J. Zhang, G. Yang and W. Zhang, *J. Am. Chem. Soc.*, 2017, **139**, 9819–9822; (*g*) L. Wei, S.-M. Xu, Q. Zhu, C. Che and C.-J. Wang, *Angew. Chem., Int. Ed.*, 2017, **56**, 12312–12316; (*h*) L. Wei, Q. Zhu, S.-M. Xu, X. Chang and C.-J. Wang, *J. Am. Chem. Soc.*, 2018, **140**, 1508–1513; (*i*) X. Huo, J. Zhang, J. Fu, R. He and W. Zhang, *J. Am. Chem. Soc.*, 2018, **140**, 2080–2084; (*j*) X. Jiang, P. Boehm and J. H. Hartwig, *J. Am. Chem. Soc.*, 2018, **140**, 1239–1242; (*k*) Z.-T. He, X. Jiang and J. H. Hartwig, *J. Am. Chem. Soc.*, 2019, **141**, 13066–13073; (*l*) L. Wei, Q. Zhu, L. Xiao, H.-Y. Tao and C.-J. Wang, *Nat. Commun.*, 2019, **10**, 1594; (*m*) Q. Zhang, H. Yu, L. Shen, T. Tang, D. Dong, W. Chai and W. Zi, *J. Am. Chem. Soc.*, 2019, **141**, 14554–14559; (*n*) R. He, X. Huo, L. Zhao, F. Wang, L. Jiang, J. Liao and W. Zhang, *J. Am. Chem. Soc.*, 2020, **142**, 8097–8103; (*o*) L. Peng, Z. He, X. Xu and C. Guo, *Angew. Chem., Int. Ed.*, 2020, **59**, 14270–14274; (*p*) S. Singha, E. Serrano, S. Mondal, C. G. Daniliuc and F. Glorius, *Nat. Catal.*, 2020, **3**, 48–54; (*q*) M. Zhu, Q. Zhang and W. Zi, *Angew. Chem., Int. Ed.*, 2021, **60**, 6545–6552; (*r*) S.-Q. Yang, Y.-F. Wang, W.-C. Zhao, G.-Q. Lin and Z.-T. He, *J. Am. Chem. Soc.*, 2021, **143**, 7285–7291; (*s*) B. Kim, Y. Kim and S. Y. Lee, *J. Am. Chem. Soc.*, 2021, **143**, 73–79; (*t*) R. Jiang, L. Ding, C. Zheng and S.-L. You, *Science*, 2021, **371**, 380–386; (*u*) J. Zhang, X. Huo, J. Xiao, L. Zhao, S. Ma and W. Zhang, *J. Am. Chem. Soc.*, 2021, **143**, 12622–12632; (*v*) L. Xiao, L. Wei and C.-J. Wang, *Angew. Chem., Int. Ed.*, 2021, **60**, 24930–24940; (*w*) Y. Peng, X. Hong, Y. Luo, L. Wu and W. Zhang, *Angew. Chem., Int. Ed.*, 2021, **60**, 24941–24949.

13 For other selected strategies for stereodivergent synthesis, see: (*a*) S.-L. Shi, Z. L. Wong and S. L. Buchwald, *Nature*, 2016, **532**, 353–356; (*b*) D. Kaldre, I. Klose and N. Maulide, *Science*, 2018, **361**, 664–667; (*c*) H. Zheng, Y. Wang, C. Xu, X. Xu, L. Lin, X. Liu and X. Feng, *Nat. Commun.*, 2018, **9**, 1968; (*d*) T.-T. Gao, W.-W. Zhang, X. Sun, H.-X. Lu and B.-J. Li, *J. Am. Chem. Soc.*, 2019, **141**, 4670–4677; (*e*) X. Liu, S. Jin, W.-Y. Zhang, Q.-Q. Liu, C. Zheng and S.-L. You, *Angew. Chem., Int. Ed.*, 2020, **59**, 2039–2043; (*f*) D.-X. Zhu, J.-G. Liu and M.-H. Xu, *J. Am. Chem. Soc.*, 2021, **143**, 8583–8589; (*g*) X. Hu, X. Tang, X. Zhang, L. Lin and X. Feng, *Nat. Commun.*, 2021, **12**, 3012; (*h*) S. Ge, W. Cao, T. Kang, B. Hu, H. Zhang, Z. Su, X. Liu and X. Feng, *Angew. Chem., Int. Ed.*, 2019, **58**, 4017–4021; (*i*) C. Xu, K. Wang, D. Li, L. Lin and X. Feng, *Angew. Chem., Int. Ed.*, 2019, **58**, 18438–18442; (*j*) C. Xu, J. Qiao, S. Dong, Y. Ahou, X. Liu and X. Feng, *Chem. Sci.*, 2021, **12**, 5458–5463.

14 S.-M. Xu, L. Wei, C. Shen, L. Xiao, H.-Y. Tao and C.-J. Wang, *Nat. Commun.*, 2019, **10**, 5553.

15 During the preparation of this manuscript, with arylidene/alkylidene aminomalonates as the precursors of non-prochiral AMYs, Deng documented an Ir-catalyzed asymmetric (3 + 4) cycloaddition of 4-indolyl allylic alcohols to generate only *cis*-isomeric azepino[3,4,5-cd] indoles bearing two stereogenic centers, see: W.-L. Yang, T. Ni and W.-P. Deng, *Org. Lett.*, 2021, **23**, 588–594. However, the reported catalytic system was unable to realize the stereodivergent preparation of azepino[3,4,5-*cd*] indoles bearing three stereogenic centers, and prochiral aldimine esters are not compatible with such a single-catalyst protocol due to the unsatisfactory diastereoselectivity control.

16 Q. Cheng, H.-F. Tu, C. Zheng, J.-P. Qu, G. Helmchen and S.-L. You, *Chem. Rev.*, 2019, **119**, 1855–1969.

17 M. Saifuddin, P. K. Agarwal, S. K. Sharma, A. K. Mandadapu, S. Gupta, V. K. Harit and B. Kundu, *Eur. J. Org. Chem.*, 2010, 5108–5117.

18 (*a*) Y. Cai, N. Shao, H. Xie, Y. Futamura, S. Panjikar, H. Liu, H. Zhu, H. Osada and H. Zou, *ACS Catal.*, 2019, **9**, 7443–7448; (*b*) D. Robaa, C. Enzensperger, S. A. Abul, E. E. Khawass, O. E. Sayed and J. Lehmann, *J. Med. Chem.*, 2010, **53**, 2646–2650; (*c*) J. S. Scott, A. Bailey, D. Buttar, R. J. Carbajo, J. Curwen, P. R. J. Davey, R. D. M. Davies, S. L. Degorce, C. Donald, E. Gangl, R. Greenwood, S. D. Groombridge, T. Johnson, S. Lamont, M. Lawson, A. Lister, C. J. Morrow, T. A. Moss, J. H. Pink and R. Polanski, *J. Med. Chem.*, 2019, **62**, 1593–1608; (*d*) X. Xiong, H. Yuan, Y. Zhang, J. Xu, T. Ran, H. Liu, S. Lu, A. Xu, H. Li, Y. Jiang, T. Lu and Y. Chen, *J. Mol. Struct.*, 2015, **1097**, 136–144; (*e*) J. Kraxner, H. Hubner and P. Gmeiner, *Arch. Pharm.*, 2000, **333**, 287–292.

19 (*a*) R. Connon and P. J. Guiry, *Tetrahedron Lett.*, 2020, **61**, 151696–151705; (*b*) T. Nemoto, S. Harada and M. Nakajima, *Asian J. Org. Chem.*, 2018, **7**, 1730–1742.

20 D.-J. Cheng, H.-B. Wu and S.-K. Tian, *Org. Lett.*, 2011, **13**, 5636–5639.

21 (*a*) J. F. Teichert and B. L. Feringa, *Angew. Chem., Int. Ed.*, 2010, **49**, 2486–2528; (*b*) C. J. Richards and A. W. Mulvaney, *Tetrahedron: Asymmetry*, 1996, **7**, 1419–1430.

22 R. Wang, X. Hong and Z. Shan, *Tetrahedron Lett.*, 2008, **49**, 636–639.

23 CCDC 2090369 ((6*S*,7*S*,9*R*)-**3a**), 2090370 ((6*R*,7*R*,9*R*)-**3a**), and 2090371 ((6*R*,7*S*,9*R*)-**3a**) contain the supplementary crystallographic data for this paper.

24 Y. Zhao, L. Liu, W. Sun, J. Lu, D. McEachern, X. Li, S. Yu, D. Bernard, P. Ochsenein, V. Ferey, J.-C. Carry, J. R. Deschamps, D. Sun and S. Wang, *J. Am. Chem. Soc.*, 2013, **135**, 7223–7234.

25 All calculations were performed using the Gaussian 09 software package: M. J. Frisch, G. W. Trucks, H. B. Schlegel, G. E. Scuseria, M. A. Robb, J. R. Cheeseman, G. Scalmani, V. Barone, B. Mennucci, G. A. Petersson, H. Nakatsuji, M. Caricato, X. Li, H. P. Hratchian, A. F. Izmaylov, J. Bloino, G. Zheng, J. L. Sonnenberg, M. Hada, M. Ehara, K. Toyota, R. Fukuda, J. Hasegawa, M. Ishida, T. Nakajima, Y. Honda, O. Kitao, H. Nakai, T. Vreven, J. A. Montgomery Jr, J. E. Peralta, F. Ogliaro, M. Bearpark, J. J. Heyd, E. Brothers, K. N. Kudin, V. N. Staroverov, T. Keith, R. Kobayashi, J. Normand, K. Raghavachari, A. Rendell, J. C. Burant, S. S. Iyengar, J. Tomasi, M. Cossi, N. Rega, J. M. Millam, M. Klene, J. E. Knox, J. B. Bakken, V. Cross, C. Adamo, J. Jaramillo, R. Gomperts, R. E. Stratmann, O. Yazyev, A. J. Austin, R. Cammi, C. Pomelli, J. W. Ochterski, R. L. Martin, K. Morokuma, V. G. Zakrzewski, G. A. Voth, P. Salvador, J. J. Dannenberg, S. Dapprich, A. D. Daniels, O. Farkas, J. B. Foresman, J. V. Ortiz, J. Cioslowski and D. J. Fox, *Gaussian 09*, Gaussian, Inc., Wallingford, CT, 2013.

26 Y. Zhao and D. G. Truhlar, *J. Chem. Phys.*, 2006, **125**, 194101–194118.

27 Selected mechanistic studies on stereodivergent dual transition metal catalysis: (*a*) A. Changotra, B. Bhaskararao, C. M. Hadad and R. B. Sunoj, *J. Am. Chem. Soc.*, 2020, **142**, 9612–9624; (*b*) H. Xu, B. Li, Z. Liu and Y. Dang, *ACS Catal.*, 2021, **11**, 9008–9021.

28 Other selected theoretical mechanistic studies on stereodivergent synergistic catalysis: (*a*) B. Bhaskararao and R. B. Sunoj, *J. Am. Chem. Soc.*, 2015, **137**, 15712–15722; (*b*) B. Bhaskararao and R. B. Sunoj, *ACS Catal.*, 2017, **7**, 6675–6685; (*c*) S. Tribedi, C. M. Hadad and R. B. Sunoj, *Chem. Sci.*, 2018, **9**, 6126–6133; (*d*) B. Bhaskararao and R. B. Sunoj, *Chem. Sci.*, 2018, **9**, 8738–8747.

29 (*a*) C. A. Kiener, C. Shu, C. Incarvito and J. F. Hartwig, *J. Am. Chem. Soc.*, 2003, **125**, 14272–14273; (*b*) J. F. Hartwig and L. M. Stanley, *Acc. Chem. Res.*, 2010, **43**, 1461–1475; (*c*) D. Marković and J. F. Hartwig, *J. Am. Chem. Soc.*, 2007, **129**, 11680–11681; (*d*) S. T. Madrahimov, D. Markovic and J. F. Hartwig, *J. Am. Chem. Soc.*, 2009, **131**, 7228–7229; (*e*) A. Leitner, S. Shekhar, M. J. Pouy and J. F. Hartwig, *J. Am. Chem. Soc.*, 2005, **127**, 15506–15514.

30 Molecular visualization was carried out in CYLview and PyMOL: (*a*) C. Y. Legault, *CYLview, 1.0b, Université de Sherbrooke: Quebec*, Montreal, Canada, 2009; (*b*) W. L. Delano, *The PyMOL molecular graphics system*, Delano Scientific, 2002.

31 P. Liu, J. Montgomery and K. N. Houk, *J. Am. Chem. Soc.*, 2011, **133**, 6956–6959.

32 Steric contours were produced in the Multiwfn code: T. Lu and F. Chen, *J. Comput. Chem.*, 2012, **33**, 580–592.

33 (*a*) S. Goncalves, S. Santoro, M. Nicolas, A. Wagner, P. Maillos, F. Himo and R. Baati, *J. Org. Chem.*, 2011, **76**, 3274–3285; (*b*) G. Alachouzos, C. Holt and A. J. Frontier, *Org. Lett.*, 2020, **22**, 4010–4015; (*c*) G.-P. Wang, M.-Q. Chen, S.-F. Zhu and Q.-L. Zhou, *Chem. Sci.*, 2017, **8**, 7197–7202.